Landscape of protein–protein interactions in *Drosophila* immune deficiency signaling during bacterial challenge

Hidehiro Fukuyama[a,1,2,3], Yann Verdier[b,1], Yongsheng Guan[a], Chieko Makino-Okamura[a,c], Victoria Shilova[a,c], Xi Liu[a,d], Elie Maksoud[a,d], Jun Matsubayashi[a], Iman Haddad[b], Kerstin Spirohn[e], Kenichiro Ono[f,g], Charles Hetru[c,d], Jean Rossier[b,4], Trey Ideker[f,g], Michael Boutros[e], Joëlle Vinh[b], and Jules A. Hoffmann[c,d,h,3]

[a]Institut National de la Santé et de la Recherche Médicale Equipe Avenir, [c]Institut de Biologie Moléculaire et Cellulaire, 67084 Strasbourg, France; [b]Spectrométrie de Masse Biologique et Protéomique, Unité de Service et de Recherche 3149, Centre National de La Recherche Scientifique, École Supérieure de Physique et de Chimie Industrielles ParisTech, 75231 Paris Cedex 05, France; [d]University of Strasbourg, 67000 Strasbourg, France; [e]German Cancer Research Center (DKFZ), Division of Signaling and Functional Genomics, and Department for Cell and Molecular Biology, Faculty of Medicine Mannheim, University of Heidelberg, 69120 Heidelberg, Germany; Departments of [f]Bioengineering and [g]Medicine, University of California, San Diego, La Jolla, CA 92093; and [h]University of Strasbourg Institute for Advanced Study, 67000 Strasbourg, France

Contributed by Jules A. Hoffmann, April 16, 2013 (sent for review February 19, 2013)

The *Drosophila* defense against pathogens largely relies on the activation of two signaling pathways: immune deficiency (IMD) and Toll. The IMD pathway is triggered mainly by Gram-negative bacteria, whereas the Toll pathway responds predominantly to Gram-positive bacteria and fungi. The activation of these pathways leads to the rapid induction of numerous NF-κB–induced immune response genes, including antimicrobial peptide genes. The IMD pathway shows significant similarities with the TNF receptor pathway. Recent evidence indicates that the IMD pathway is also activated in response to various noninfectious stimuli (i.e., inflammatory-like reactions). To gain a better understanding of the molecular machinery underlying the pleiotropic functions of this pathway, we first performed a comprehensive proteomics analysis to identify the proteins interacting with the 11 canonical members of the pathway initially identified by genetic studies. We identified 369 interacting proteins (corresponding to 291 genes) in heat-killed *Escherichia coli*-stimulated *Drosophila* S2 cells, 92% of which have human orthologs. A comparative analysis of gene ontology from fly or human gene annotation databases points to four significant common categories: (*i*) the NuA4, nucleosome acetyltransferase of H4, histone acetyltransferase complex, (*ii*) the switching defective/sucrose nonfermenting-type chromatin remodeling complex, (*iii*) transcription coactivator activity, and (*iv*) translation factor activity. Here we demonstrate that sumoylation of the IκB kinase homolog immune response-deficient 5 plays an important role in the induction of antimicrobial peptide genes through a highly conserved sumoylation consensus site during bacterial challenge. Taken together, the proteomics data presented here provide a unique avenue for a comparative functional analysis of proteins involved in innate immune reactions in flies and mammals.

IMD interactome | functional proteomics | small ubiquitin-like modifier

Innate immune responses are common among metazoans, and it is now understood that the basic molecular machineries of these responses evolved early in evolution and have been well conserved.

The model organism *Drosophila* has provided significant insights into these defenses. A hallmark of innate immunity in the fly is the challenge-induced production of several families of distinct, mostly small-sized membrane active peptides/polypeptides with various activity spectra directed against bacteria and fungi. This production is dependent on two intracellular signaling cascades that control the expression of antimicrobial peptide genes (and of hundreds of other immune response genes) via members of the NF-κB family of inducible transactivators (1): (*i*) The Toll pathway, which is predominantly activated during fungal and Gram-positive bacterial infections, and (*ii*) the immune deficiency (IMD) pathway, which was initially identified by its role in the defense against Gram-negative bacteria. However, it has become apparent that this pathway, which shares significant similarities with the mammalian TNF receptor pathway (1), can also be activated by noninfectious stimuli (i.e., inflammatory-like reactions). Indeed, Mukae et al. and our group (2, 3) revealed that flies carrying a hypomorphic mutation in the *DNaseII* (*DNaseII*^{lo}) constitutively expressed the IMD-dependent *Attacin A*, but not the Toll-dependent *Drosomycin* gene.

To date, forward genetic and genome-wide RNA interference (RNAi) screens have identified 11 canonical molecules in the IMD pathway reviewed in ref. 4. In short, during activation of this pathway, the bacteria sensors peptidoglycan recognition protein (PGRP)-LC (transmembrane type) and/or PGRP-LE (intracellular type) recruit the adaptor molecule IMD (which shows some degree of similarity to mammalian receptor interacting protein 1) to form a complex with Fas-associated death domain (FADD) and death-related ced-3/neural precursor cell expressed developmentally downregulated 2 (NEDD2)-like protein (DREDD; equivalent to mammalian caspase 8/10); this leads to the activation of the mitogen-activated protein 3 (MAP3) kinase TGF β-activated kinase 1 (TAK1) and eventually to that of the IκB kinase (IKK) complex, IKKβ/immune response-deficient 5 (IRD5) and IKKγ/Kenney (KEY). This complex subsequently activates the NF-κB family member Relish (Rel), which is cleaved by the caspase DREDD, allowing for nuclear translocation of the Rel homology domain.

This simplified scheme, however, leaves many questions unanswered. We reasoned that to get a better understanding of the IMD pathway, additional information was required about the protein complexes formed between and around the canonical pathway members. For this, we undertook a pathway-wide and

Author contributions: H.F., K.O., C.H., J.R., T.I., and J.A.H. designed research; H.F., Y.V., Y.G., X.L., E.M., J.M., I.H., K.S., and J.V. performed research; H.F., C.M.-O., and V.S. contributed new reagents/analytic tools; H.F., Y.V., Y.G., X.L., M.B., and J.V. analyzed data; and H.F. and J.A.H. wrote the paper.

The authors declare no conflict of interest.

Freely available online through the PNAS open access option.

Data deposition: All proteins and protein–protein interactions have been deposited in the ProteomeXchange Consortium via the PRIDE partner repository, http://proteomecentral.proteomexchange.org/ [dataset ID code PXD000129 (DOI 10.6019/PXD000129)].

[1]H.F. and Y.V. contributed equally to this work.

[2]Present address: Laboratory for Lymphocyte Differentiation, RIKEN Center for Integrative Medical Sciences, Tsurumi-ku, Yokohama, Kanagawa 230-0045, Japan.

[3]To whom correspondence may be addressed. E-mail: j.hoffmann@unistra.fr or hidehiro.fukuyama@riken.jp.

[4]Present address: Optogenetics and Brain Imaging, Centre de Psychiatrie et Neurosciences, Institut National de la Santé et de la Recherche Médicale U894, Faculté de Médecine, Université Paris Descartes, 2ter rue d'Alésia, 75014 Paris, France.

This article contains supporting information online at www.pnas.org/lookup/suppl/doi:10.1073/pnas.1304380110/-/DCSupplemental.

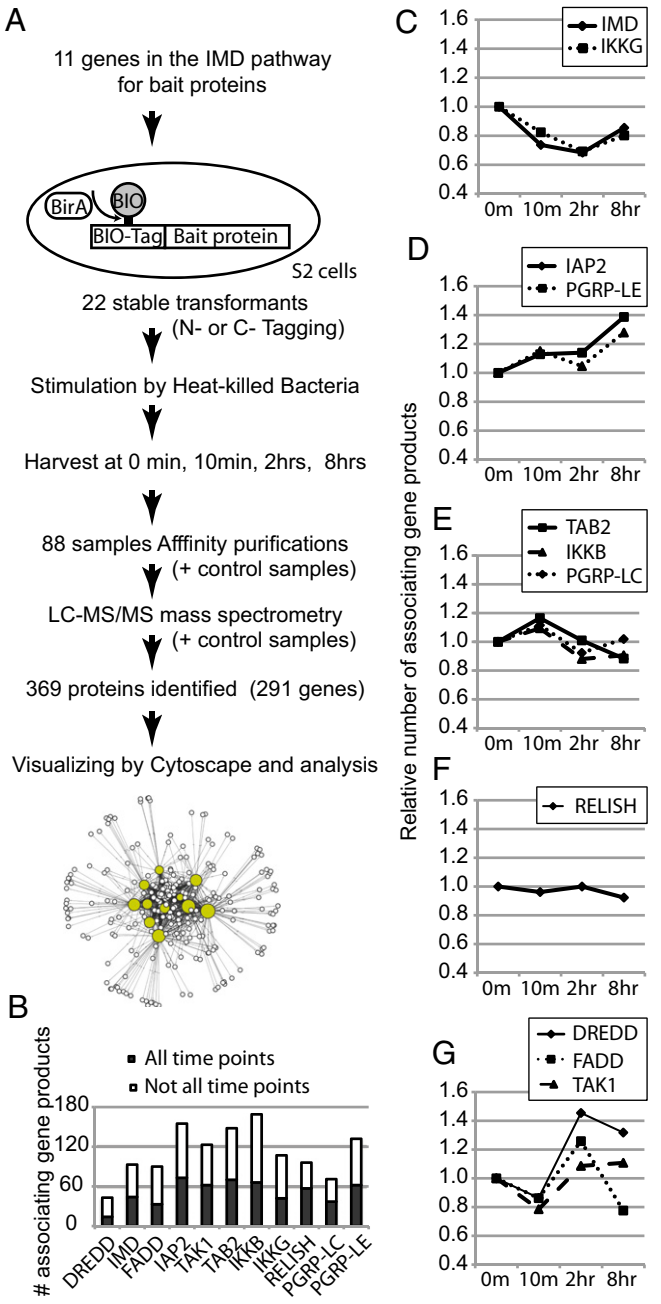

Fig. 1. Overview of the functional proteomics analysis of the IMD pathway. (*A*) Work flow of the experiment. Light green nodes represent the bait proteins. The size of nodes is in relation to the numbers of interactants. (*B*) Number of identified proteins per bait. Black columns indicate the numbers of proteins found at all time points, and white columns indicate those found at some time points only. (*C*–*G*) Fold-change of numbers of identified proteins over time in each bait. Numbers of identified proteins at 0 min is considered the base.

time-lapse proteomics approach aimed at identifying all interacting proteins in S2 cells challenged by heat-killed *Escherichia coli*. This approach led us to identify 369 interacting proteins, corresponding to 291 genes. Knockdown experiments of the corresponding genes by RNAi indicates that approximately half of the genes affect the induction of antimicrobial peptide reporter genes following bacterial challenge in S2 cells. This dataset will provide the basis for an in-depth analysis of the molecular events underlying the roles of the IMD pathway in host reaction to microbial challenge or to noninfectious stimuli, illustrated below in one example where we unexpectedly noted that IκB kinase homolog IRD5 is sumoylated at a site highly conserved between *Drosophila* and mammals, and that this sumoylation is required for the induction of the antimicrobial peptide attacin A in response to bacterial challenge.

Results

Pathway-Wide and Time-Lapse Functional Proteomics Analysis. The following 11 proteins were chosen as baits because they have previously shown to be involved in the activation of the IMD pathway: PGRP-LC, PGRP-LE, IMD, BG4 [*Drosophila* FADD (dFADD)], DREDD, TAK1, TGF-β–activated kinase 1/MAP3K7 binding protein 2 (TAB2), inhibitor of apoptosis protein 2 (IAP2), IRD5 (DmIKKβ), KEY (DmIKKγ), and Relish (4). Each protein was fused N terminally or C terminally with a biotin tag and was stably expressed in S2 cells previously subjected to stable integration of the bacterial enzyme BirA to allow for biotinylation of the tags. In total, we established 22 stable transformant cell lines (11 genes × two tag locations), which were individually stimulated by heat-killed *E. coli* before harvest at four different time points (t = 0 min, 10 min, 2 h, and 8 h; Fig. 1*A*). This procedure was followed by streptavidin-mediated affinity purification of 96 bait–protein complexes (22 transformants × four time points, plus eight unstimulated controls without baits), on-bead trypsin digestions of the protein complexes, and liquid chromatography (LC)–MS/MS analysis (5). We identified 369 proteins, and their corresponding 291 genes are visualized as the IMD pathway interactome in the open-source Cytoscape platform (6) (Fig. 1*A* and Dataset S1). Each bait–protein complex, merged from both

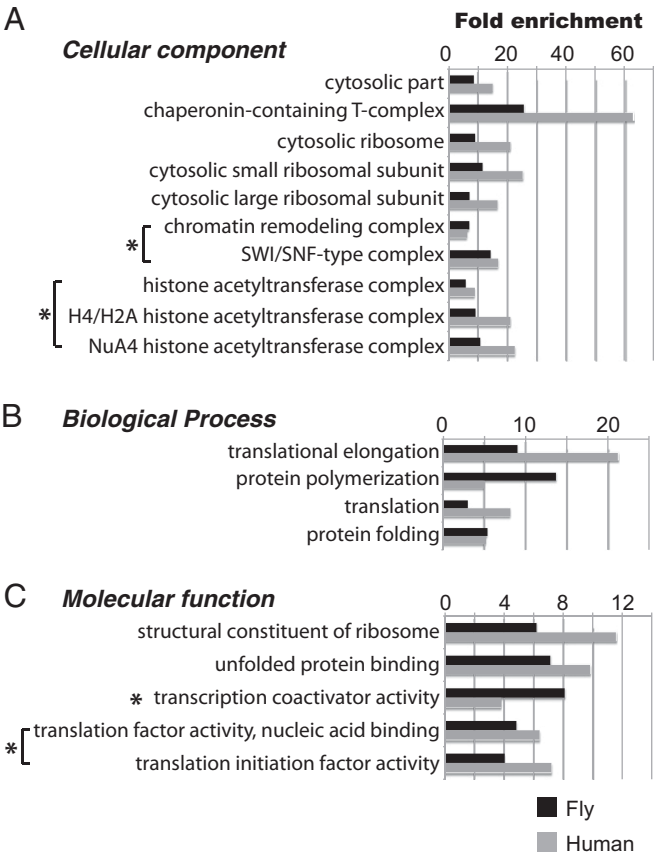

Fig. 2. Functional clusters common between humans and flies and their associated genes. GO terms of cellular components (*A*), biological processes (*B*), and molecular functions (*C*) shared between human and fly annotation databases are shown. Black and gray bars indicate fold-enrichment values for humans and flies, respectively. Four major parental GO terms are indicated with an asterisk.

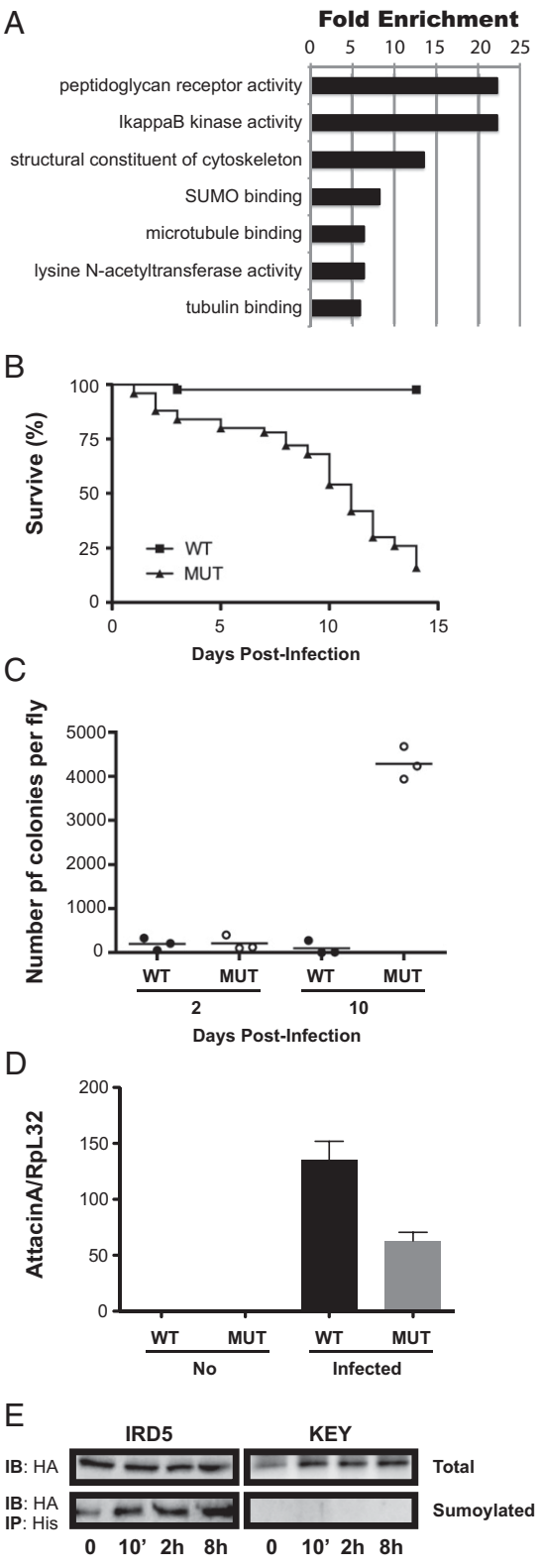

Fig. 3. Sumoylation cascade and its role in the defense against bacteria. (*A*) Ontology term enrichment in molecular function in the IMD interactome using the *Drosophila* database. (*B*) The survival of *DmUbc9* (*lwr*) mutants (MUT) during bacterial challenge (WT, $n = 43$; MUT, $n = 50$). Statistical significance: $^*P < 0.0001$ by log-rank test. (*C*) Bacterial growth over time postinfection ($n = 3$–4 per dot). Statistical significance: $^*P < 0.0001$ by two-tailed Student *t* test (WT vs. MUT at day 10). Individual experiments are shown in dots; bars indicate the average. (*D*) *Attacin A* induction 6 h postinfection. The average and SD of three independent experiments are shown. *Attacin A* expression is normalized to that of *RpL32* that encodes ribosomal protein. Statistical significance: $^*P = 0.0143$ by Student *t* test (WT vs. MUT during infection). (*E*) SMT3 is covalently linked to IRD5 but not to KEY. His-tagged SMT3 was immunoprecipitated from cells challenged by administration of heat-killed *E. coli* at 0 min (control), 10 min, 2 h, and 8 h and HA-tagged IRD5 and KEY were detected by an anti-HA antibody. Five percent of input is shown as total.

N- and C-terminal tags, contained an average of 112 proteins with values ranging from 43 for DREDD to 169 for IRD5/IKKβ (Fig. 1*C*). Interestingly, 269 of the 291 proteins identified in this interactome have human orthologs (Dataset S2). More than half of the proteins were identified only after bacterial challenge of the cells. The number of identified proteins also changed over time depending on the bait protein (Fig. 1 *C*–*G*). We tested the potential relevance of the 214 genes in the IMD pathway by two independent RNAi-mediated gene knockdown assays (*SI Materials and Methods*) and a total of 102 genes (47%) altered reporter gene activities in cells following Gram-negative bacterial challenge. As shown in Fig. S1, our results on some of the interactants and protein–protein interactions are in agreement with those found in the comprehensive *Drosophila* Interaction Database, which contains all previously known protein–protein and genetic interactions (7). For instance, both sets show that IMD, FADD, and DREDD form a complex, and that IRD5 and KEY are associated. In addition, several proteins identified previously in the context of studies on the IMD pathway were also identified in this study: KAY (Kayak), PVR (PDGF- and VEGF-receptor related), MASK (multiple ankyrin repeats single KH domain), αTUB84B (α-Tubulin at 84B), CG6509, CG4849, IntS1(Integrator 1), RPL22 (Ribosomal protein L22), OST48(Oligosaccharyltransferase 48kD subunit), EIF-2α (eukaryotic translation Initiation Factor 2α), αTUB84D (α-Tubulin at 84D), MESR4 (Misexpression suppressor of ras 4), AGO2(Argonaute 2), SCAR (suppressor of cAMP receptors), RpS27 (Ribosomal protein S27), MED14 (Mediator complex subunit 14), and SKPA (Skp1-related gene A) (8–11). Of note, the precise functions of these proteins in the IMD-dependent immune response remain largely unknown. In contrast, we were unable to identify some proteins reported recently to act as negative regulators of the IMD pathway—namely, CASP (Casper), POSH (Plenty of SH3s), DNR1 (defense repressor 1), and PIRK [poor Imd response upon knock-in; also known as RUDRA or PIMS (PGRP-LC-interacting inhibitor of Imd signaling)]. As reported recently by Lhocine et al. (12), PGRP-LCx and PIMS can become insoluble in Triton X-100 lysis conditions. Because we used Triton X-100–soluble fractions, this could be one explanation as to why some interacting proteins present in the insoluble fractions are absent from our analysis.

Possible NuA Histone Acetyltransferase and Chromatin Remodeling Functions in the Activation of the IMD Pathway. We next performed gene ontology (GO) analysis using Database for Annotation, Visualization and Integrated Discovery (DAVID) Bioinformatics Resources (13). Comparison of GO terms from fly or human gene annotation databases point to four major shared GO terms: (*i*) histone acetyltransferase complex (GO:0000123), in particular the NuA histone acetyltransferase complex subgroup, (*ii*) chromatin remodeling complex (GO:0016585), in particular the SWI/SNF-type complex subgroup, (*iii*) transcription coactivator activity binding (GO:0003713), and (*iv*) translation factor activity (GO:0008135; Fig. 2). Of particular interest, pontin [PONT; human ortholog RuvB-like 1 (Ruvbl1)], reptin [REPT; human ortholog RuvB-like 2 (Ruvbl2)], and domino [DOM; human ortholog Snf2-related CREBBP activator protein/p400 (Srcap)] are shared among the histone acetyltransferase complex and chromatin remodeling complex GO term groups. RNAi-mediated depletion of *pontin*, *reptin*, or *domino* showed a marked reduction of NF-κB reporter activity in S2 cells after heat-killed *E. coli* stimulation (Dataset S3).

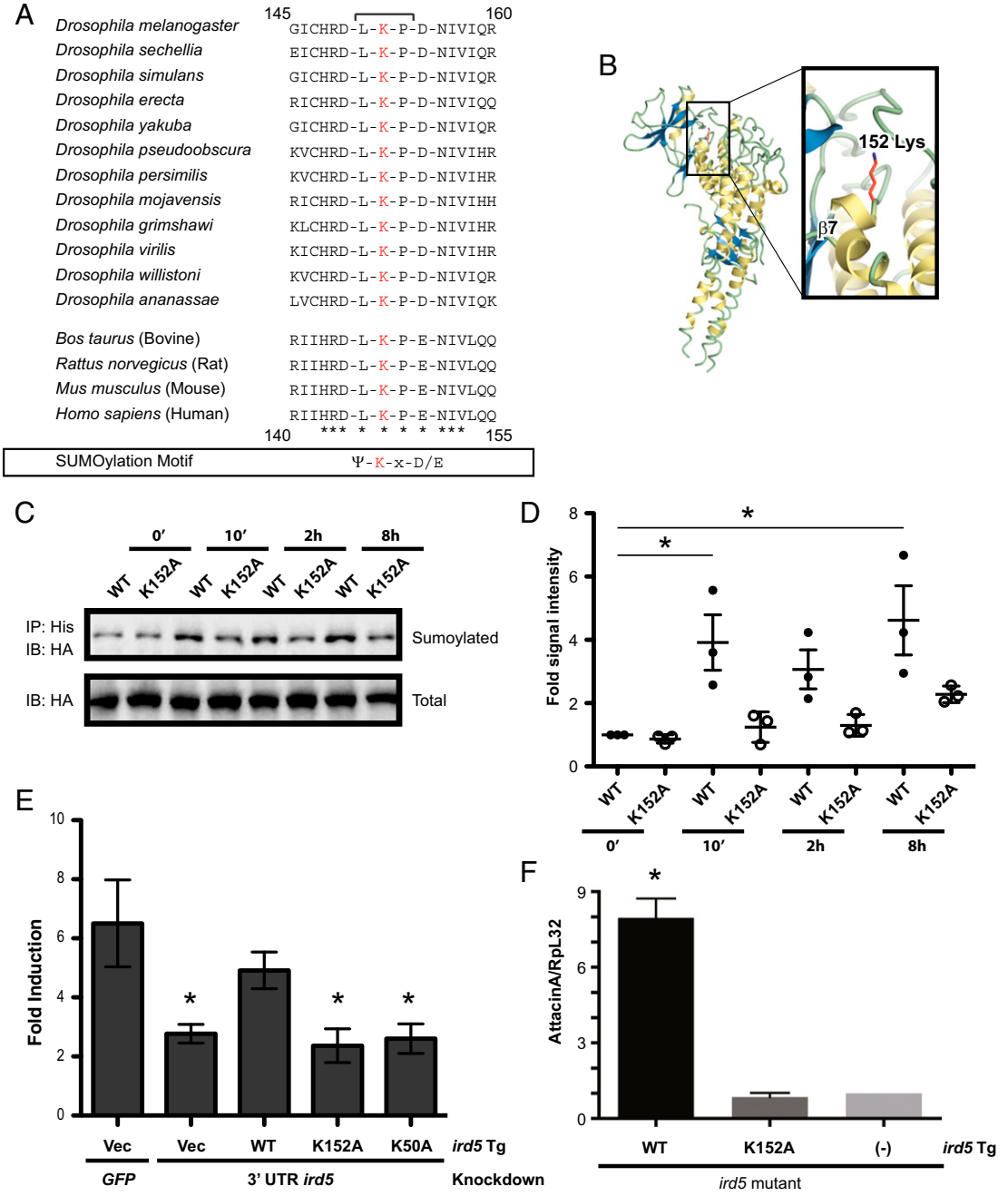

Fig. 4. K152 sumoylation of IRD5 is induced and critical for AMP induction. (*A*) Amino acid sequence alignment of the IRD5 homologs among 12 *Drosophila* species and four mammalian species. The sumoylation consensus motif is shown, Ψ-K-x-D/E: Ψ, hydrophobic amino acids; K, lysine; x, any amino acid; D/E, aspartate/glutamate. (*B*) Three-dimensional view of *Xenopus* IKKβ (PDB ID code 3RZF; visualized by CueMol). Orange-colored side chain (*Inset*) indicates lysine at amino acid position 152 (20). (*C*) K152 of IRD5 is sumoylated in a stimulation-dependent manner. His-tagged SMT3 was immunoprecipitated from cells transfected with WT vs. K152A IRD5 constructs and challenged by administration of heat-killed *E. coli* at 0 min (control), 10 min, 2 h, and 8 h; HA-tagged IRD5 WT and IRD5 K152A were detected by anti-HA antibody. Five percent of input is shown as total. (*D*) A time-dependent analysis of the levels of sumoylation in cells transfected with WT vs. K152A IRD5 constructs and challenged by administration of heat-killed *E. coli* at 0 min (control), 10 min, 2 h, and 8 h. The value observed at 0 min for WT constructs was set as 1 on the scale. The average and SD from three experiments are shown. One-way ANOVA was performed ($P = 0.0009$) and followed by Dunnett's multiple comparison test. Asterisks indicate statistical significance ($P < 0.05$) compared with WT at 0 min. (*E*) IRD5 WT constructs restore *Attacin A* induction, but not the SUMO-mutant and kinase-dead forms. S2 cells were transfected with either *GFP* dsRNA as negative control or 3′ UTR *ird5* dsRNA and various forms of *ird5* (K152A, SUMO mutant; K50A, kinase dead) were individually expressed. Firefly luciferase activities of the reporter *Attacin A* firefly luciferase were measured and normalized to *Renilla* luciferase activities of *Act5C-Renilla* luciferase. The relative value against nonstimulated cells is shown. The value represents the average and SD from three independent experiments. One-way ANOVA was performed ($P = 0.0003$) and followed by Dunnett's multiple comparison test. Asterisks indicate statistical significance ($P < 0.05$) compared with Vec/GFP:GFP dsRNA knockdown; empty vector transfection. (*F*) In vivo rescue experiment. *Ird5* WT or K152A transgenic flies in an *ird5*-deficient background were established using ΦC31 transgenesis. Flies were challenged by live *E. coli*. The *Attacin A* mRNA level was measured by quantitative RT-PCR and normalized to *RpL32*. The relative values are indicated against nontransgenic *ird5* mutants. Each value represents the average with SD, from three independent experiments. A pool of 5–7 adult flies per genotype was collected in each experiment. One-way ANOVA was performed ($P < 0.0001$) and followed by Dunnett's multiple comparison test. Asterisk indicates statistical significance ($P < 0.05$) compared with nontransgenic *ird5* mutants.

PONT and REPT belong to the AAA+ (ATPase associated with diverse cellular activities) family of ATPases and are part of chromatin remodeling complexes (14). Recent studies have implicated these molecules in various cellular processes, including transcription, DNA damage response, small nucleolar RNA (snoRNA) assembly, and cancer metastasis (15). Our data indicate that PONT and REPT are constitutively present in the IKK complex.

In *Drosophila*, DOM is a SWI2/SNF2 class chromatin-remodeling ATPase and has a role in the exchange between the phosphorylated and unphosphorylated forms of the H2Av histone variant in nucleosomal arrays during DNA damage (16). H2AX, the mammalian equivalent of *Drosophila* H2Av, can be acetylated by TIP60 (the catalytic subunit of NuA4-type HAT complex) before H2A exchange by DOM; H2AX is subsequently polyubiquitinated by UBC13, an E2 ubiquitin-conjugating enzyme (17). Interestingly, in our dataset, DOM is associated only transiently at 2 h with IAP2, a protein with ubiquitin E3 ligase activity. Of note, in mammals the precise mechanism of NuA4 (TIP60) HAT complex-mediated activation of NF-κB during bacterial challenge is still not understood.

Small Ubiquitin-Like Modifier Modification of the IKK Complex. Pending an in-depth analysis of the precise functions of the various interactants found in this study, we chose to focus here on the relevance of the molecular function GO term "SUMO binding" in Fig. 3*A*. Indeed, we observed that small ubiquitin-like modifier (SUMO) proteins are associated with IRD5 (IKKβ) and KEY (IKKγ) in the *Drosophila* IKK complex. To examine the role of sumoylation in IMD signaling, we addressed a well-characterized loss-of-function missense mutant of the *lesswright* (*lwr*; alternatively, *DmUbc9*) gene, in which an Arg is changed to a His at position 104 of the E2 SUMO conjugation enzyme DmUBC9; UBC9 facilitates the addition of the SUMO protein (SMT3) to proteins in *Drosophila*. Because the homozygous *lwr* mutants are lethal (18), we infected heterozygote *lwr* flies with live *E. coli* and noted that these flies succumbed to infection (Fig. 3*B*). Consistently, bacterial growth in heterozygote *lwr* flies was drastically increased compared with wild-type at day 10 postinfection (Fig. 3*C*). Furthermore, the expression of the antibacterial peptide gene *Attacin A*, one of the representative target genes of NF-κB in the IMD pathway, was significantly reduced in heterozygote *lwr* flies (Fig. 3*D*). These results reveal that sumoylation plays an important role in IMD-dependent immune responses against bacteria. Sumoylation is a posttranslational protein modification that contributes to many facets of the functional regulation of proteins, such as kinase activity, subcellular localization, and protein–DNA binding (19). We next stably expressed HA-tagged IRD5 and KEY, together with polyhistidine-tagged SMT3, and performed affinity purification of sumoylated proteins in denaturing conditions followed by immunoblot using anti-HA antibodies. We found that IRD5 is sumoylated, but not KEY (Fig. 3*E*). Using our experimental conditions, we observed that the majority of IRD5 is monosumoylated (Fig. S2).

K152 Is a Functional Sumoylation Site. Amino acid sequence alignment of the IRD5 homologs of 12 *Drosophila* species and several mammalian species followed by prediction of sumoylation sites using Web-based bioinformatics software SUMOsp 2.0 (http://sumosp.biocuckoo.org) led us to identify a putative sumoylation motif Ψ-K-x-D/E around K152. Of the four potential sumoylation sites of IRD5, the K152 motif is conserved among all *Drosophila* species and in many vertebrate species; this motif is shared with the IKK family member IKKα in mammals (Fig. 4*A*). Note that *Drosophila* IK2, and its mammalian orthologs TBK1 and IKKε, do not have this lysine residue, although the sequence in this region is well conserved (Fig. S3). As shown in 3D structural analysis by Xu et al. (20), the K152 residue is located in the loop between two β-strands, β6 and β7 (Fig. 4*B*). We next investigated whether the sumoylation consensus sequence in IRD5 is indeed sumoylated, and, if so, what functional relevance it would assert in NF-κB activation. For this, we used *Drosophila* cell lines stably expressing polyhistidine-tagged SMT3 and either HA-tagged WT or mutated (K152A) IRD5. Cells were stimulated with heat-killed *E. coli*, and proteins were extracted followed by immunoprecipitation and immunoblotting. Fig. 4 *C* and *D* show that WT IRD5 is increasingly sumoylated over time; sumoylation of the mutated form (K152A) remains at the level of unstimulated cells. We next analyzed the relevance of K152 sumoylation of IRD5 on NF-κB activation. For this, we knocked down *ird5* by RNAi and observed that the level of induction of the reporter gene was lowered by 50% compared with controls. We then transfected the *ird5* knockdown cells with one of the three following IRD5 constructs: (*i*) WT, (*ii*) the SUMO-mutant form (K152A), or (*iii*) the kinase-dead form (K50A) (21). Significantly, only WT IRD5 could restore the loss of reporter gene expression observed in the *ird5* knockdown cells (Fig. 4*E*). The expression of different forms of *ird5* did not alter the level of induction (Fig. S4). Furthermore, we established *ird5* transgenic fly lines expressing either WT or K152A in an *ird5*-deficient background. Six hours after injecting Gram-negative bacteria into these flies, we observed that only the WT construct could support the induction of endogenous *Attacin A* in contrast to K152A (Fig. 4*F*). These data indicate that K152 sumoylation of IRD5 plays a pivotal role in NF-κB activation in vivo and in vitro.

Discussion

Our studies on the IMD interactome revealed multiple potential regulators of IMD pathway activation. IRD5 sumoylation is one method of regulation. In support of this, another SUMO-related molecule, VELOREN, exists in our IMD interactome dataset. VELOREN is the *Drosophila* ortholog of mammalian sentrin-specific protease 6 (SENP6), which functions for desumoylation (22). It still remains to be understood why IRD5 needs to be sumoylated upon bacterial challenge. It is well accepted that mammalian IKKβ functions as a regulator of NF-κB activation. However, there is an interesting observation that during UV irradiation, NF-κB can be activated by IκBα degradation without IKKβ-mediated phosphorylation (23, 24). Recently, Tsuchiya et al. (25) revealed that nuclear IKKβ is an adaptor protein for IκBα ubiquitination and degradation. It will be interesting to investigate whether K152 sumoylation of IKKβ is also important for the function of mammalian IKKβ and, if so, in what circumstances IKKβ sumoylation is required for activation of NF-κB.

Our interactome dataset contains ribosomal protein S3 (RPS3). Wan et al. (26) identified RPS3, a KH domain protein, as a non-Rel subunit that associates with the Rel protein p65 to regulate key genes in rapid cellular activation responses. Furthermore, Sen et al. (27) recently revealed that sulfhydration of p65 at a conserved cysteine 38 is important for association with the coactivator RPS3, DNA binding, and antiapoptotic gene expression. Interestingly, the food-borne pathogen *E. coli* strain O157:H7 has acquired a mechanism that enables it to specifically inhibit phosphorylation of RPS3 Ser209, subsequently blocking RPS3 function; phosphorylation promotes nuclear localization of RPS3 upon a lymphocyte-activating stimulus (28).

We also identified *cindr*, the *Drosophila* ortholog of CIN85 and CD2AP. CINDR has three SH3 domains and positively regulates receptor-mediated endocytosis (29). Kometani et al. (30) demonstrated that CIN85 functions upstream of IKKβ in the activation of NF-κB in B cells and is responsible for T-cell–independent type II antibody responses in vivo.

Of further interest are chromatin remodeling and histone acetyltransferase activities linked to the activation of the IMD pathway. Chromatin remodeling complexes are classified into four distinct families (14): switching defective/sucrose nonfermenting (SWI/SNF); imitation switch (ISWI); chromodomain, helicase, DNA binding (CHD); and inositol requiring 80 (INO80). Our interactome dataset contains SWI/SNF and INO80 family members. In the SWI/SNF family, we identified most of the components of the SWI/SNF remodeler complex, such as MOR (human

BAF155, BAF170), BAP60 (human BAF60 a, b, or c), SNR1 (human SNF5/BAF47/INI1), BAP55 (human BAF53a or b), and ACTIN (human β-actin). This family has multiple activities, including the sliding and ejecting of nucleosomes. Limpert et al. (31) reported that BRG1, the core helicase of the mammalian SWI/SNF remodeling complex, is required for Schwann cells to differentiate and to form myelin through a complex with NF-κB. In the INO80 family, we found DOMINO (human SRCAP), REPTIN (human Ruvbl1), PONTIN (human RuvBl2), BAP55 (human BAF53a), ACTIN 87E (human actin), DMAP1 (human DMAP1), and MRG15 (human MRG15 or MRGX) categorized into a Tip60-type complex. This complex has diverse functions. For example, the SWR1 (Swi2/SNF-related 1, the yeast complex equivalent to *Drosophila* Tip60) complex can replace the canonical H2A–H2B histone dimers with variant H2A.Z–H2B dimers, subsequently altering nucleosome structure to regulate transcription and DNA repair. *Drosophila domino* mutants show developmental defects in their blood cells (i.e., hemocytes) (32). Similarly, *mDomino* (alternatively, *Ep400*) knockout mice show defects in embryonic and adult bone marrow hematopoiesis (33, 34). Recently, Arnold et al. (35) isolated a mouse *Ruvbl2* mutant named *Worker*. *Worker* heterozygous mutants show a delay in T-dependent humoral immune responses together with a defect in T-cell development (35). It will be important to reveal how the Tip60 complex regulates NF-κB activation, in addition to its roles in hematopoietic cell development (35).

We anticipate that the data provided above will serve as a basis for further in-depth analyses of the highly conserved regulatory network of the IMD pathway. The roles of many of the interactant proteins presented in the figures have remained elusive to date, and their functions will have to be established both in the antimicrobial defense and in the inflammatory-like reactions such as those noted in *DNaseII*-deficient flies (2, 3).

In conclusion, unexpectedly large numbers of proteins that associate with the IMD interactome were identified in our study. Interestingly, over 90% of these proteins have human orthologs. We cannot firmly exclude that some of the 300 interactants could result from accidental protein–protein interactions. However, in the RNAi knockdown results, close to 50% of the interactants have a phenotype by simply looking at the expression of *Attacin A*; we are confident that most of the data in this study present functional interactions. With this large data set, it is reasonable to expect that understanding precise functions of molecules identified in this study will provide more insights into defense reactions and provide beneficial targets for fighting human diseases.

Materials and Methods

Eleven genes in the *Drosophila* IMD pathway, *PGRP-LCx*, *PGRP-LE*, *imd*, *FADD*, *Dredd*, *Iap2*, *Tab2*, *Tak*, *key*, *ird5*, and *Rel*, were chosen for functional proteomics. Individual genes were N- or C-tagged with a biotin tag and stably expressed in BirA-expressing *Drosophila* S2 cells (Fig. S5). Cells of each clone were harvested at four different time points (t = 0 min, 10 min, 2 h, and 8 h). The protein complex was affinity purified from the supernatant of each lysate and on-bead tryptic digested. Peptides were purified on a capillary reverse-phase column, and the MS analysis was performed on a Fourier transform ion cyclotron resonance (FT-ICR) mass spectrometer (LTQ-FT Ultra; ThermoFisher Scientific), followed by MS/MS (linear trap quadrupole). Proteome Discoverer 1.3 (ThermoFisher Scientific) and Mascot were used to search the data and filter the results. Protein–protein interactions were visualized by Cytoscape open-source software. The DAVID version 6.7 was used for our GO studies. Statistical analysis was performed using GraphPad Prism software. All primers used in this study are listed in Dataset S4. Extended materials and methods can be found in *SI Materials and Methods*.

ACKNOWLEDGMENTS. We thank T. Furuyama, A. Cohen, and H. Stunnenberg for technical advice on the BirA system; S. Ozkan for transgenesis; S. Estelle, L. Kleitz, and T. Rhinn-Tanaka for technical assistance; and V. Wolf and S. Risch for administrative support. We also thank the Bloomington Stock Center for providing fly stocks; F. G. Grosveld for providing the BirA plasmid; and W.-J. Lee for providing pPAC-His-DLAK WT and K50A plasmids. This work was supported by Institut National de la Santé et de la Recherche Médicale Young Investigator Avenir Grant (to H.F.), BioMalPar (J.A.H.), National Institutes of Health Grant P01 AI070167 (to J.A.H.), the Balzan Foundation (J.A.H.), and Centre National de la Recherche Scientifique through the TGE FT-ICR for conducting mass spectrometry (J.V., I.H., and Y.V.).

1. Hoffmann JA (2003) The immune response of Drosophila. *Nature* 426(6962):33–38.
2. Mukae N, Yokoyama H, Yokokura T, Sakoyama Y, Nagata S (2002) Activation of the innate immunity in Drosophila by endogenous chromosomal DNA that escaped apoptotic degradation. *Genes Dev* 16(20):2662–2671.
3. Liu X, et al. (2012) Drosophila EYA regulates the immune response against DNA through an evolutionarily conserved threonine phosphatase motif. *PLoS ONE* 7(8):e42725.
4. Ferrandon D, Imler JL, Hetru C, Hoffmann JA (2007) The Drosophila systemic immune response: Sensing and signalling during bacterial and fungal infections. *Nat Rev Immunol* 7(11):862–874.
5. Fukuyama H, et al. (2012) On-bead tryptic proteolysis: An attractive procedure for LC-MS/MS analysis of the Drosophila caspase 8 protein complex during immune response against bacteria. *J Proteomics* 75(15):4610–4619.
6. Cline MS, et al. (2007) Integration of biological networks and gene expression data using Cytoscape. *Nat Protoc* 2(10):2366–2382.
7. Murali T, et al. (2011) DroID 2011: A comprehensive, integrated resource for protein, transcription factor, RNA and gene interactions for Drosophila. *Nucleic Acids Res* 39(Database issue):D736–D743.
8. Foley E, O'Farrell PH (2004) Functional dissection of an innate immune response by a genome-wide RNAi screen. *PLoS Biol* 2(8):E203.
9. Kleino A, et al. (2005) Inhibitor of apoptosis 2 and TAK1-binding protein are components of the Drosophila Imd pathway. *EMBO J* 24(19):3423–3434.
10. Gesellchen V, Kuttenkeuler D, Steckel M, Pelte N, Boutros M (2005) An RNA interference screen identifies Inhibitor of Apoptosis Protein 2 as a regulator of innate immune signalling in Drosophila. *EMBO Rep* 6(10):979–984.
11. Khush RS, Cornwell WD, Uram JN, Lemaitre B (2002) A ubiquitin-proteasome pathway represses the Drosophila immune deficiency signaling cascade. *Curr Biol* 12(20):1728–1737.
12. Lhocine N, et al. (2008) PIMS modulates immune tolerance by negatively regulating Drosophila innate immune signaling. *Cell Host Microbe* 4(2):147–158.
13. Huang W, Sherman BT, Lempicki RA (2009) Systematic and integrative analysis of large gene lists using DAVID bioinformatics resources. *Nat Protoc* 4(1):44–57.
14. Clapier CR, Cairns BR (2009) The biology of chromatin remodeling complexes. *Annu Rev Biochem* 78:273–304.
15. Jha S, Dutta A (2009) RVB1/RVB2: Running rings around molecular biology. *Mol Cell* 34(5):521–533.
16. Gévry N, Chan HM, Laflamme L, Livingston DM, Gaudreau L (2007) p21 transcription is regulated by differential localization of histone H2A.Z. *Genes Dev* 21(15):1869–1881.
17. Ikura T, et al. (2007) DNA damage-dependent acetylation and ubiquitination of H2AX enhances chromatin dynamics. *Mol Cell Biol* 27(20):7028–7040.
18. Apionishev S, Malhotra D, Raghavachari S, Tanda S, Rasooly RS (2001) The Drosophila UBC9 homologue lesswright mediates the disjunction of homologues in meiosis I. *Genes Cells* 6(3):215–224.
19. Hay RT (2005) SUMO: A history of modification. *Mol Cell* 18(1):1–12.
20. Xu G, et al. (2011) Crystal structure of inhibitor of κB kinase β. *Nature* 472(7343):325–330.
21. Kim YS, et al. (2000) Lipopolysaccharide-activated kinase, an essential component for the induction of the antimicrobial peptide genes in Drosophila melanogaster cells. *J Biol Chem* 275(3):2071–2079.
22. Berdnik D, Favaloro V, Luo L (2012) The SUMO protease Verloren regulates dendrite and axon targeting in olfactory projection neurons. *J Neurosci* 32(24):8331–8340.
23. Bender K, Göttlicher M, Whiteside S, Rahmsdorf HJ, Herrlich P (1998) Sequential DNA damage-independent and -dependent activation of NF-kappaB by UV. *EMBO J* 17(17):5170–5181.
24. Li N, Karin M (1998) Ionizing radiation and short wavelength UV activate NF-kappaB through two distinct mechanisms. *Proc Natl Acad Sci USA* 95(22):13012–13017.
25. Tsuchiya Y, et al. (2010) Nuclear IKKbeta is an adaptor protein for IkappaBalpha ubiquitination and degradation in UV-induced NF-kappaB activation. *Mol Cell* 39(4):570–582.
26. Wan F, et al. (2007) Ribosomal protein S3: A KH domain subunit in NF-kappaB complexes that mediates selective gene regulation. *Cell* 131(5):927–939.
27. Sen N, et al. (2012) Hydrogen sulfide-linked sulfhydration of NF-κB mediates its antiapoptotic actions. *Mol Cell* 45(1):13–24.
28. Wan F, et al. (2011) IKKβ phosphorylation regulates RPS3 nuclear translocation and NF-κB function during infection with *Escherichia coli* strain O157:H7. *Nat Immunol* 12(4):335–343.
29. Quinones GA, Jin J, Oro AE (2010) I-BAR protein antagonism of endocytosis mediates directional sensing during guided cell migration. *J Cell Biol* 189(2):353–367.
30. Kometani K, et al. (2011) CIN85 drives B cell responses by linking BCR signals to the canonical NF-kappaB pathway. *J Exp Med* 208(7):1447–1457.
31. Limpert AS, et al. (2013) NF-κB forms a complex with the chromatin remodeler BRG1 to regulate Schwann cell differentiation. *J Neurosci* 33(6):2388–2397.
32. Braun A, Lemaitre B, Lanot R, Zachary D, Meister M (1997) Drosophila immunity: Analysis of larval hemocytes by P-element-mediated enhancer trap. *Genetics* 147(2):623–634.
33. Fujii T, Ueda T, Nagata S, Fukunaga R (2010) Essential role of p400/mDomino chromatin-remodeling ATPase in bone marrow hematopoiesis and cell-cycle progression. *J Biol Chem* 285(39):30214–30223.
34. Ueda T, et al. (2007) Critical role of the p400/mDomino chromatin-remodeling ATPase in embryonic hematopoiesis. *Genes Cells* 12(5):581–592.
35. Arnold CN, et al. (2012) A forward genetic screen reveals roles for Nfkbid, Zeb1, and Ruvbl2 in humoral immunity. *Proc Natl Acad Sci USA* 109(31):12286–12293.